Journal of Power Sources 196 (2011) 4136–4142

Contents lists available at ScienceDirect

Journal of Power Sources

journal homepage: www.elsevier.com/locate/jpowsour

Composite $LiFePO_4$/AC high rate performance electrodes for Li-ion capacitors

N. Böckenfeld, R.-S. Kühnel, S. Passerini*, M. Winter, A. Balducci**

Westfälische Wilhelms Universität, Institut für Physikalische Chemie, Corrensstr. 28/30, 48149 Münster, Germany

ARTICLE INFO

Article history:
Received 25 August 2010
Received in revised form 29 October 2010
Accepted 7 November 2010
Available online 12 November 2010

Keywords:
Lithium-ion capacitors
$LiFePO_4$
AC
CMC
Aqueous processing

ABSTRACT

This manuscript reports the performance of composite electrodes based on the mixture of two, electrochemically active, materials: lithium iron phosphate ($LiFePO_4$) and activated carbon (AC). The sodium salt of carboxymethylcellulose (CMC) was used as binder to cast the composite electrodes out of aqueous slurries. The investigated electrodes display high specific capacity and high cycling stability. Upon constant current tests with a charge rate of 50C and a discharge rate of 1D, the electrodes display a capacity of ca. 70 mAh g^{-1} while 60 mAh g^{-1} are delivered during pulse sequence tests at 100C. These results indicate such electrodes as promising candidates for the realization of lithium-ion capacitors.

1. Introduction

The development of electrochemical devices able to display at the same time high energy and power densities as well as high cycling stability certainly represents a challenge. In the last years several strategies have been investigated in order to realize such systems. Among them, the combination of a lithium-ion battery electrode with a supercapacitor electrode appears as one of the most promising. Because of the combination of these two different electrodes, such devices, which can be defined as lithium-ion capacitors, can display energy and power density values in between those of lithium-ion batteries and supercapacitors with a satisfactory cycling stability [1].

An interesting approach in view of a further development of a lithium-ion capacitor consists in extending the material combination within the same electrode, i.e. to realize composite electrodes containing at the same time active materials used in lithium-ion batteries and in supercapacitors [2,3]. Considering the electrode materials currently used in these technologies, an appealing choice for the application of this approach consists in the realization of electrodes containing lithium iron phosphate ($LiFePO_4$) and activated carbons (ACs). $LiFePO_4$, in fact, displays high capacity stability during prolonged cycling, good rate performance, environment friendliness, low cost, and safety [4–6]. ACs, on the other hand, are the most common materials for supercapacitors because of their low cost, large capacitance and excellent cycle stability. Moreover, ACs display the advantage of being easily processable [7]. Taking into account these properties, the realization of composite electrodes containing both these active materials could represent a viable strategy to develop electrodes with high energy density, high cycling stability and the ability to be charged and discharged at high currents.

Recently, we showed that the introduction of CMC as binder for $LiFePO_4$-based electrodes is a viable and extremely promising solution to improve the overall electrode preparation since, among other advantages, it permits the use of aqueous slurries without any negative effect on the electrode performance [8]. In a recent work the possibility of using CMC as the binder for AC-based double layer supercapacitors has been proven feasible in terms of performance [9]. Considering the intrinsic safety and the low price of $LiFePO_4$, AC and CMC, the development of composite electrodes based on these components is certainly very attractive in view of the development of greener, safer and cheaper lithium-ion capacitors.

This manuscript is focused on the study of the performance of a composite electrode containing $LiFePO_4$ and AC as active materials and CMC as binder. In the first part of the paper, the influence of the conducting agent content on the rate capability of $LiFePO_4$-based electrodes using CMC as binder is reported. In fact, $LiFePO_4$, even if coated with a thin layer of carbon, does not display very high conductivity, thus the rate capability of $LiFePO_4$-based composite electrodes is strongly affected by the amount of conducting agent present in the composite electrode [10,11]. Also, most of the commercial ACs do not display conductivities as high as those of conducting agents commonly used for the preparation of composite electrodes used in lithium-ion batteries. Therefore, in order to realize high rate performance composite electrodes containing $LiFePO_4$

* Corresponding author.
** Corresponding author. Tel.: +49 2518336083; fax: +49 2512518336084.
E-mail addresses: stefano.passerini@uni-muenster.de (S. Passerini), andrea.balducci@uni-muenster.de (A. Balducci).

0378-7753/$ – see front matter © 2010 Elsevier B.V. All rights reserved.
doi:10.1016/j.jpowsour.2010.11.042

Table 1
Specific surface area (BET) and average particle size of the electrode components.

	Specific surface area (BET) ($m^2\ g^{-1}$)	Average particle size μm
$LiFePO_4$ (wt.%)	14	0.5–1
Super P (wt.%)	62	0.04
DLC Super 30 (wt.%)	1400	6.3

Table 2
Electrode compositions.

	Electrode I	Electrode II	Electrode III	Electrode IV
$LiFePO_4$ (wt.%)	85	75	65	65
Super P (wt.%)	10	20	30	10
DLC Super 30 (wt.%)	0	0	0	20
CMC (wt.%)	5	5	5	5

and AC, the content of conducting agent inside the electrodes needs to be carefully addressed [12].

In the second part of the paper, the performance of composite electrodes containing $LiFePO_4$ and AC is compared with that of $LiFePO_4$-based electrodes. The aim of this comparison is the understanding of the role played by AC inside the electrode and the evaluation of the advantages in terms of electrode performance contributed by the AC.

Finally, the performance of the electrode containing $LiFePO_4$ and AC during pulse tests (up to 100C rate) and during charge–discharge cycles at very high charge rate (50C) is reported.

2. Experimental

Carbon-coated $LiFePO_4$ was provided by a commercial supplier (Südchemie, Germany) and used as delivered. The activated carbon (DLC Super 30) was provided by Norit Activated Carbon. Sodium carboxymethyl-cellulose (CMC) was provided by Dow Wolff Cellulosics (Walocel CRT 2000 PPA 12) with a degree of substitution of 1.2. As conducting agent Super P (TIMCAL) was used.

The BET specific surface area of the electrode components was determined from N_2 adsorption experiments. The Super P and DLC Super 30 materials were characterized by N_2 adsorption at 77 K using a Micromertrics model ASAP-2020 analyzer. The materials were degassed for 12 h at 633 K to remove moisture or other adsorbed species from the surface. The BET surface area was calculated by the software delivered from the Micromertrics Instrument Corporation Version 3.03 by applying the BET equation to the adsorption data. The BET specific surface area of the $LiFePO_4$ and the average particle sizes of the Super P and $LiFePO_4$ were given by the respective manufacturers. The average particle size of the DLC Super 30 and $LiFePO_4$ was determined by diffraction/scattering particle size analysis with a Cilas particle size analyzer (model 1064) in an aqueous suspension. The specific surface area, the average particle size of $LiFePO_4$, Super P and DLC Super 20 are reported in Table 1.

For the preparation of the electrodes CMC was dissolved in high purity deionized water by magnetic stirring for 1 h at room temperature, to obtain a 1.5 wt.% solution. The required amounts of Super P, $LiFePO_4$ and activated carbon (the latter only when needed) were then added and the mixture was further homogenized for one more hour by magnetic stirring. The slurry was then dispersed with a high energy stirrer (Ultra-Turrax®, IKA) for 1 h. The so-obtained slurry was casted immediately on aluminium foil (30 μm, purity > 99.9%, etched by immersion in 5 wt.% KOH at 60 °C for 30 s) by using a laboratory scale doctor blade coater, whose blade was set to a wet film thickness of 100 μm. The coated electrode was immediately pre-dried in an atmospheric oven with stagnant air at 80C for 12 h. Disc electrodes with a diameter of 12 mm were cut from the so-obtained electrode tapes. The disc electrodes were dried at 170 °C under vacuum for 24 h. Four different electrode compositions are considered in this paper, which are reported in Table 2. The average mass loading of all electrodes was 2.3 mg cm^{-2}. All electrode were used "as prepared" meaning without any post treatment (e.g. roll pressing). All the electrochemical tests were carried out with 3-electrode Swagelok®-type cells. The cells were assembled in an Argon-filled glove box with oxygen and water contents lower than 1 ppm. Metallic lithium (Chemetall) was used for both the counter and the reference electrodes. As electrolytic layer, a stack of polypropylene fleeces (Freudenberg FS2190) drenched with 120 μL of electrolyte was used. The electrolyte used in all tests was 1 M $LiPF_6$ in propylene carbonate (PC). The water content of the electrolytic solution was less than 10 ppm.

The density of the electrodes was quantified by measuring the area, thickness and composite material mass loading of the electrodes.

The electronic conductivity of the electrodes was evaluated by impedance spectroscopy on the electrodes coated on aluminium foil. In order to decrease the contact resistance, a gold layer was sputtered in vacuum two times for 300 s at a bias current of 45 mA on the open face of the electrodes. To avoid electrical contact between the gold film and the aluminium current collector a mask was applied so that only a disc of 4.5 mm radius in the centre of the electrodes was covered with gold. The electrodes were contacted with two polished steel current collector in a two electrode configuration. Impedance measurements were carried out with a Solartron model 1260 Impedance/Gain-Phase Analyzer between 1 MHz and 1 Hz at an AC amplitude of 10 mV. The resistance of the electrodes was calculated from the impedance measurements at the lower frequencies, where a negligible phase shift (phase angle $\theta < 1$) was observed which results in the complex impedance being equal to the resistive impedance ($R = |Z| \cos\theta$). The impedance data processing was performed with the ZPlot® Software by Scribner Associates Inc.

All electrochemical tests were performed at room temperature (20 °C ± 2 °C) with a MACCOR Battery tester 4300.

All potential values quoted in this paper refer to the Li/Li^+ reference electrode. The cut-off voltages of 4.2 V and 2.8 V were set for the charge and discharge processes, respectively, independent of the test procedure used. Note that "C/*n*" means that the charge current is set up to achieve the nominal capacity (calculated assuming the $LiFePO_4$ as the only active material) in "*n*" hours. The same rule applies to the discharge steps where "D/*n*" corresponds to a discharge in "*n*" hours (e.g. 10C corresponds to a charge in 6 min; 10D corresponds to a discharge in 6 min).

Two different kinds of rate performance tests were carried out. In the discharge rate tests a constant rate of C/10 (ca. 0.04 mA cm^{-2}) was applied while the discharge rate was varied from D/10 (ca. 0.04 mA cm^{-2}) to 5D (ca. 2.0 mA cm^{-2}). In the charge rate test a constant rate of D/10 (ca. 0.04 mA cm^{-2}) was used while the charge rate was varied from C/10 (ca. 0.04 mA cm^{-2}) to 20 C (ca. 8.0 mA cm^{-2}).

Constant current (CC) tests were performed by applying current densities corresponding to 1C–5D, 5C–1D and 50C–1D.

Pulse tests were carried out using different test protocols. In the first pulse test protocol (PT1), 20 1C–1D cycles were initially carried out. After these cycles, the electrodes were charged using pulses of 1 s followed by a relaxation time of 4 s until the cut-off potential of 4.2 V was reached. After that, the electrodes were discharged with a current density corresponding to 1D. This charge–discharge protocol was repeated three times. After that, the electrodes were subjected to three cycles at 1C–1D. This sequence of three pulsed and three non-pulsed cycles was repeated with increasing pulse current densities. The pulse current density was

varied from 2.0 mA cm^{-2} (corresponding to 5C) to 20 mA cm^{-2} (corresponding to 50C).

In the second pulse test protocol (PT2), 20 1C–1D cycles were initially carried out. After these cycles, the electrodes were charged using pulses (100 ms and 400 ms relaxation time) with a current density of 40 mA cm^{-2} (corresponding to 100C) until the cut-off potential of 4.2 V was reached. After that, the electrodes were discharged with a current density corresponding to 1D. This 100C (pulsed)–1D test protocol was repeated for 100 cycles. Finally, three cycles at 1C–1D rate were carried out to ascertain the electrode capacity.

3. Results and discussion

In order to understand the relationship between the conducting agent content and the rate capability of $LiFePO_4$-based electrodes, the performance of electrodes containing 10, 20 and 30 wt.% of Super P (indicated in Table 1 as I, II and III, respectively) was investigated.

Fig. 1a shows the rate performance recorded during the tests performed at various discharge rates ranging from D/10 (ca. 0.04 mA cm^{-2}) to 5D (ca. 2.0 mA cm^{-2}) and charged a C/10 rate, while Fig. 1b shows the rate performance recorded during the tests performed at various charge rates ranging from C/10 (ca. 0.04 mA cm^{-2}) to 20C (ca. 8.0 mA cm^{-2}) and discharged at D/10. The use of different maximum rates in the two tests is related with the observed reduction of capacity shown by the electrodes during the tests. In practice the increase of the C/D-rate was ended when the delivered capacity was 35–40% lower than that recorded during the C/10–D/10 cycle (i.e., the first cycle). To facilitate the comparison, both figures report the discharge capacity values as obtained directly in the test at various D rates or considering the D/10 discharges following each charge in the test at the various C rates. All capacity values are given with respect to the amount of $LiFePO_4$ in the electrodes.

As shown in Fig. 1a, during the discharge rate test, the performance of the three electrodes is quite similar. At D/10 all electrodes displayed capacity slightly above 140 mAh g^{-1} and no major differences were observed upon a discharge rate increase up to 5D. When different charge rates were used, however, the electrodes displayed a different behaviour. As shown in Fig. 1b, the charge performance of all electrodes is comparable from low to medium-high charging rates (from C/10 to 10C). However, at 20C the initial capacity of electrode I is reduced by 40%, while in the case of the electrodes II and III the reduction of capacity is less dramatic.

The results of these tests indicate that $LiFePO_4$-based electrodes show a different ability to sustain high current densities during the charge and discharge processes. As reported earlier, a 25% reduction with respect to the D/10 rate capacity is observed at a discharge rate of 5D. In the charging process, however, a comparable reduction is obtained at current rates four times higher (20C). The existence of an asymmetric behaviour between charge and discharge in $LiFePO_4$-based electrodes has been already reported by Srinivasan and Newman [13]. In their work, the authors show that under current densities where transport limitation are important (e.g. starting form 3C), the electrode capacity is considerably higher during the charge than during the discharge process.

It is obvious that at high current rate (starting from 10C) the higher content of conducting agent improves the electrode performance. However, it is interesting to note that during charge at high rate the specific capacity between the electrodes II and III is very similar. This similar behaviour is most likely related with the differences in term of conductivity and density of these two electrodes. As indicated in Table 3, the electrode III displays slightly higher conductivity but considerably lower density with respect to the electrode II. During test at high rate, the low density of electrode III is probably affecting the performance of this electrode because of the higher electrode thickness, which results in a longer ionic path into the electrolyte filling the electrode pores. To the contrary, electrode II probably displays a favourable compromise between electronic conductivity and density (i.e. short ionic path in the pore electrolyte) and, for that reason, is able to offer a good performance at high rates.

Table 3
Density and electrical conductivity of the electrodes.

	Density (g cm^{-3})	Electronic conductivity (S cm^{-1}
Electrode I	1.21	4.2×10^{-3}
Electrode II	0.80	7.5×10^{-3}
Electrode III	0.48	8.5×10^{-3}
Electrode IV	0.67	3.4×10^{-2}

The performance of the electrodes was also investigated in terms of cycle stability during constant current (CC) cycling tests. Initially, all electrodes were subjected to 100 cycles at 1C–5D rates. After these initial cycles, the electrodes were subjected to additional 500 cycles with the same conditions (1C–5D; Fig. 2a) or the opposite conditions (5C–1D; Fig. 2b).

As shown in Fig. 2a, all electrodes displayed excellent cycling stability over 500 cycles independent of the Super P content. Practically, no capacity fading was observed during the test. Nevertheless, it can be seen from the figure, that during these tests the Super P content appeared to affect the electrode performance more sharply than during the previously shown D-rate tests (Fig. 1). As a matter of fact, the electrode I displayed a capacity about 70 mAh g^{-1}, while the electrodes II and III displayed capacities of about 100 mAh g^{-1}. This difference can only be ascribed to the effect of the Super P additive on the electrodes subjected to both, charge and discharge moderate rates.

In Fig. 2b are shown the results obtained from the electrodes upon application of the 5C–1D test. As shown in the figure, during these tests all electrodes displayed a significantly higher capacity, with respect to the results illustrated in Fig. 2a. Electrode I displayed a capacity of more than 100 mAh g^{-1}, which is nearly 43% higher than that obtained for the same electrode using the 1C–5D test. Electrodes II and III also showed the same enhancement in term of specific capacity. Like in the case of the tests reported in Fig. 1, the higher electrode capacity observed during the tests at 5C–1D is to be ascribed to the asymmetric behaviour of $LiFePO_4$ electrode during charge and discharge at high current rates [13].

In both CC tests, all electrodes displayed high capacity retention. Independent on the electrode composition the average capacity fading was lower than 0.02% per cycle. Nevertheless, the 5C–1D rate test seems to affect the cycling stability slightly more than the 1C–5D rate test, although it can be considered most favourable to obtain high value of specific capacity.

To summarize the results of these preliminary tests, it is evident that Super P plays a major role only during very high rate charge tests (>5C) and moderate charge discharge tests (1C–5D). Thus, it was considered that a very high Super P content in the composite electrode was not really necessary in the $LiFePO_4$/AC where the AC component would always contribute to the overall electronic conductivity. Mixed active material, composite electrodes, which composition was 65 wt.% $LiFePO_4$, 20 wt.% AC, 10 wt.% Super P and 5 wt.% CMC (indicated as electrode IV in Table 1), were realized. To verify if the addition of the activated carbon would have a positive effect on the electrode performance the same tests described above were executed on electrodes IV and their performance is compared with that of electrodes III, which have the same content of $LiFePO_4$.

As reported in Fig. 3, electrodes IV displayed a capacity 15% higher than that of the electrodes III in both rate performance tests.

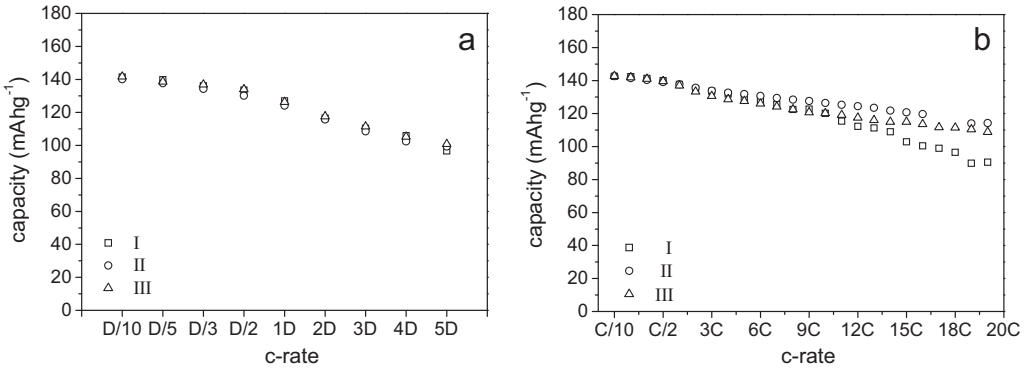

Fig. 1. Rate performance of $LiFePO_4$ electrodes containing different amounts of Super P. The tests were performed at various rates ranging from D/10 (ca. 0.04 mA cm^{-2}) to 5D (2.0 mA cm^{-2}) and C/10 (panel a) and charge rates ranging from C/10 to 20C (8 mA cm^{-2}) and D/10 (panel b). The electrode compositions are reported in Table 1.

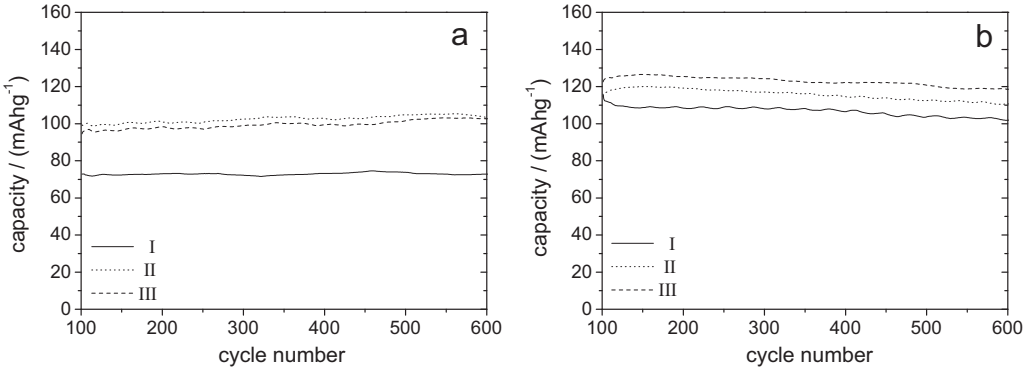

Fig. 2. Long-term cycling performance tests of $LiFePO_4$ electrodes containing different amounts of Super P. The tests were performed at 1C–5D rate (panel a) and at 5C–1D rate (panel b). The electrode compositions are reported in Table 1.

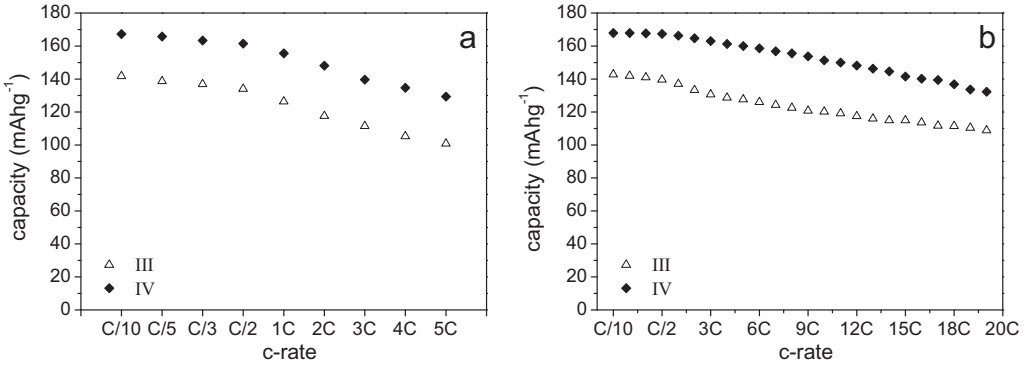

Fig. 3. Comparison of the rate performance of a $LiFePO_4$ (III) electrode with that of a $LiFePO_4$/AC (IV) electrode. The tests were performed at various discharge rates ranging from D/10 (ca. 0.04 mA cm^{-2}) to 5D (2.0 mA cm^{-2}) and C/10 (panel a) and various charge rates ranging from C/10 to 20C (8 mA cm^{-2}) and D/10 (panel b). The electrode compositions are reported in Table 1.

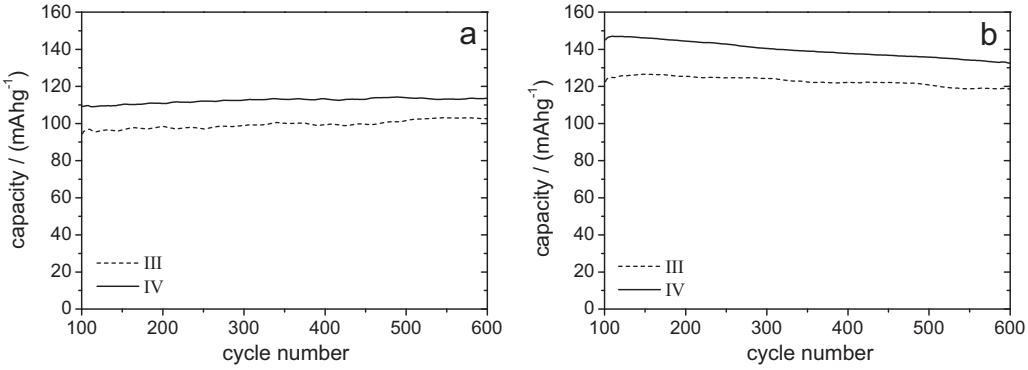

Fig. 4. Comparison of the long-term cycle performance tests of a $LiFePO_4$ (III) electrode and a $LiFePO_4$/AC (IV) electrode. The tests were performed at 1C–5D rate (panel a) and at 5C–1D rate (panel b). The electrode compositions are reported in Table 1.

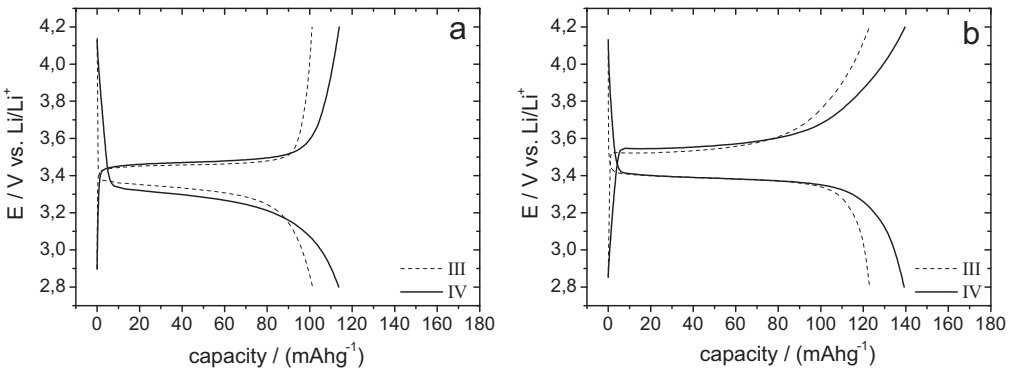

Fig. 5. Voltage profiles recorded during the 250th cycle of a $LiFePO_4$ (III) electrode and a $LiFePO_4$/AC (IV) electrode. The voltage profiles are related to the data indicated in Fig. 4. The tests were performed at 1C–5D rate (panel a) and at 5C–1D rate (panel b).

At C/10–D/10 the electrodes IV exhibited a specific capacity higher than 165 mAh g^{-1}. Upon the D-rate test, the electrodes displayed a specific capacity of 130 mAh g^{-1} at 5D (Fig. 3a) while for increasing charge rates their specific capacity was 130 mAh g^{-1} at 20C (Fig. 3b). These values are always 15% higher than those displayed by the electrode III in the same test condition, thus indicating that, however, the two electrodes display comparable reduction of capacity within the investigated C-rate as well as D-rate ranges. Nevertheless, a significant difference in term of specific capacity between the electrodes IV and III exists, which is also observed upon CC cycling tests. As shown in Fig. 4, where the results of the constant current (1C–5D) test are reported, the electrode IV displayed, once more, a capacity about 15% higher than that of the electrode III (110 mAh g^{-1} vs. 95 mAh g^{-1}) without any substantial capacity fade. In the 5C–1D testing protocol, the observed difference in specific capacity between the electrodes IV and III was even higher. The electrodes IV displayed an initial capacity of 150 mAh g^{-1}, which is 20% higher than that of the electrode III. Nevertheless, electrode IV displayed a slight capacity fading (lower than 0.02% per cycle) over cycling as seen earlier for all other electrodes.

Fig. 5 shows the charge and discharge voltage profiles of the electrodes III and IV as recorded during the 250th cycle of the 1C–5D (see Fig. 5a) and 5C–1D (see Fig. 5b) tests reported in Fig. 4. The addition of 20 wt.% AC resulted in a significant change of the voltage profile during both tests. During the discharge process at 5D (Fig. 5a), the voltage profile of the electrode IV appears to be different from that of electrode III. At the beginning of the discharge, in fact, the typical capacitive discharge profile of AC is clearly observed, which contributed for about 4.4 mAh g^{-1} to the overall electrode capacity. This value corresponds well to the capacity that would be delivered by a pure AC electrode (data not shown) in the voltage range between 4.2 V and 3.4 V (ca. 20 mAh g^{-1} corresponding to 6 mAh g^{-1} of $LiFePO_4$). On continuing the discharge process, electrodes IV displayed a plateau located at slightly lower potential than that of electrodes III. However, this shift of the voltage plateau did not negatively affect the specific capacity of the electrode. At the end of the discharge the overall capacity gain of electrode IV with respect to electrode III is about 15 mAh g^{-1}, which is higher than the capacity that would be delivered by a pure AC electrode (data not shown) in the voltage range between 4.2 V and 2.8 V (ca. 35 mAh g^{-1} corresponding to 10 mAh g^{-1} of $LiFePO_4$).

Upon the 5C–1D test, the difference between electrodes IV (20 wt.% AC) and electrodes III is even more evident (see Fig. 5b). The contribution of AC is strongly visible during the discharge, and also during the charge process. The AC offered a contribution to the electrode capacity in the order of 3–4 mAh g^{-1} of $LiFePO_4$ for the 5C as well as for the 1D process. In particular, at the beginning of the 1D process between 4.2 V and 3.44 V the AC contribution of 3.2 mAh g^{-1} is observed. The same is true for the 5C process, where the AC contribution in the same order of magnitude (about 3.8 mAh g^{-1}) can be observed in the voltage range between 2.8 V and 3.5 V. In this test, the overall capacity offered by the electrode IV is almost 20 mAh g^{-1} higher than that of electrode III.

While it is clear that AC is an active component in these electrodes, and, as such, it increased the specific capacity of the electrode, it is also very interesting to notice that its contribution to the electrode capacity cannot justify completely the 20% increase in specific capacity with respect to the electrodes containing only Super P. As a matter of fact, when the values of capacity reported in Fig. 3 for the electrodes IV and III are compared, the difference in capacity is always more than 3–5 mAh g^{-1}, which would be the contribution to the capacity of the AC that can be estimated from the profiles of Fig. 5. During the 1C–5D test the difference of capacity between the two electrodes was almost 15 mAh g^{-1}. In the case of the 5C–1D test this difference was even higher and the electrode IV showed almost 20 mAh g^{-1} more capacity than electrode III. To understand the reason of this substantial increase of performance it is useful to compare the values of conductivity and density of electrodes IV and III. As indicated in Table 2, electrode IV displays a considerably higher conductivity and also a higher density with respect to electrode III (3.4×10^{-2} S cm^{-1} and 0.67 g cm^{-3} vs. 8.5×10^{-3} S cm^{-1} and 0.49 g cm^{-3} for IV and III, respectively). AC displays an average particle size much bigger than Super P (6.3 μm vs. 0.04 μm for AC and Super P, respectively), as reported in Table 1. Previous studies showed that in $LiFePO_4$ composite electrodes, the combination of conductive agent with other carbon-based materials with different size and conductivity (e.g. carbon-fiber and multi-wallet carbon nanotubes) can provide a highly conductive network around the active materials particle and thus improve the electrode performance [14,15]. Considering these results, it is reasonable to suppose that the presence of small (Super P) and big (AC) particles around the $LiFePO_4$ in the composite electrode IV is able to create a highly conductive network around the active material particles which leads to an increment of the electronic conductivity of the electrode. At the same time, the replacement of parts of Super P with AC leads to an increase of the electrode density. Both, the increased electronic conductivity and electrode density contribute to the favourable performance of electrode IV. In fact, both the higher electronic and ionic conductivity resulting from the shorter ionic conduction paths in the pore electrolyte increase the charge–discharge process (i.e. the electrode capacity). This effect is amplified at high charge rate where the limiting processes are the electronic and ionic conductivity in the composite electrode rather than the Li-ion diffusion in the $LiFePO_4$ particle bulk.

The performance of the $LiFePO_4$/AC electrodes indicates these electrodes as good candidate cathodes for the realization of

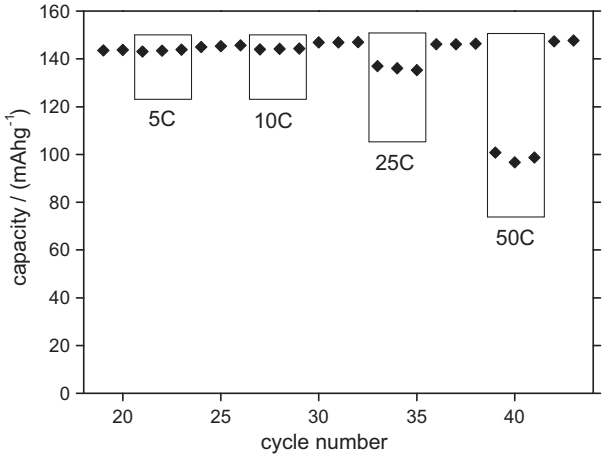

Fig. 6. Discharge capacity displayed by a $LiFePO_4$/AC electrode (IV) during the PT1 pulse test (pulse period of 1 s and relaxation time of 4 s). The pulse charge current density was varied from 2.0 mA cm^{-2} (corresponding to 5C) to 20 mA cm^{-2} (corresponding to 50C) while the discharge was always performed at 1D rate. Each sequence of pulses was followed by three cycles at 1C–1D. The capacity delivered in these 1C–1D cycles is also reported.

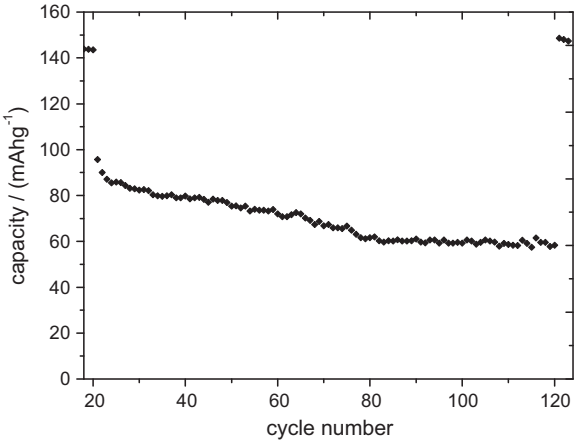

Fig. 7. Discharge capacity displayed by a $LiFePO_4$/AC electrode (IV) during the pulsed charge test (PT2). The pulse charge current density was 40 mA cm^{-2} (corresponding to 100C with a pulse period of 0.1 s and a relaxation time of 0.4 s) while the discharge was performed at 1D rate. The capacity delivered in the 1C–1D cycles performed before and after the sequence of 100 pulsed cycles is also reported.

lithium-ion capacitors. With the aim to better understand the performance of this electrode, the evaluation of the electrode rate capability during high current pulse tests was performed. Sequences of pulses (from 5C up to 50C) were applied to the electrodes following the testing protocol (PT1) described in the Section 2. Between each train of pulses, 3 cycles at 1C–1D were always carried out to verify whether the high pulse current densities negatively affected the electrodes. In Fig. 6 the discharge capacities obtained after the train of pulses and the 1C–1D cycles are shown. As indicated in the figure, during the train of pulses at 5C and 10C, the discharge capacity of the electrode is decreased by less or about than 1%, respectively. With the pulses at 25C the discharge capacity is reduced by only about 8.5% while at 50C the electrode was still able to display more than 65% of its 1C–1D capacity. These results clearly show that these electrodes are able to sustain high charge pulses without dramatic loss of capacity. Moreover, it is important to notice that the electrodes did not show any difference during the reference 1C–1D test cycles after each pulse sequence (up to 50C), thus indicating that the applied charge pulse sequence does not cause permanent degradation of the electrode performance. Taking into account this promising performance the electrode behaviour was also evaluated under a 100C pulsed charge sequence test (PT2). During this test the electrode was initially charged and discharged at 1C–1D (20 cycles). After these preliminary cycles, 100 consecutive cycles in which the electrodes were charged with 100C pulses (corresponding to ca. 40.0 mA cm^{-2} for 100 ms followed by relaxation for 400 ms) were carried out. Finally, the electrodes were cycled at 1C–1D (3 cycles) to verify whether this pulse test exerted any negative effect on the electrode. The results of this test are reported in Fig. 7. At the beginning of the pulse test the electrode displayed a specific capacity of nearly 100 mAh g^{-1}. During the pulsed charge test, the specific capacity gradually decreased to reach a stable value of ca. 60 mAh g^{-1} after sixty cycles, which was than maintained until the end of the test. After the pulse sequence test the electrode fully recovered its initial specific capacity of about 145 mAh g^{-1}. Considering these results, it is clear that this electrode can very well sustain also short pulses of 100C. Of course, this is a further positive indication in view of its application in a lithium-ion capacitor.

As a final performance test, the same $LiFePO_4$/AC electrodes used for the 100C pulsed test (PT2) were subjected to high C-rate cycles. Initially, fifty 10C–1D cycles were applied in order to "stabilize" the electrode (results not shown). Then, one hundred 50C–1D cycles were carried out. As shown in Fig. 8, after an initial decrease of capacity during the first 20 cycles the electrode displayed a stable capacity of about 70 mAh g^{-1} until the end of the cycling test. This performance is certainly very promising and indicates that this electrode can deliver high capacity even when charged at 50C. Moreover, it is interesting to note that the values of capacity obtained during the test at 50C are comparable with those observed during the pulse tests carried out at 100C (see Fig. 7). As described in the Section 2, in these two tests the charge conditions were distinctly different. During the pulses at 100C a current density of ca. 40.0 mA cm^{-2} was applied only for a short time (100 ms), while during the CC test at 50C a current density of 20.0 mA cm^{-2} is applied for more than 20 s. For that, the results of the 50C–1D test can be also seen as an indication of the ability of this electrode to sustain high current density for a long period of time and for a large number of cycles.

Work is now in progress to further investigate the performance of the electrodes containing 20 wt.% AC during CC and pulse tests at higher C-rate than those shown in this paper. Furthermore, the electrodes will be tested in combination with different electrolytes and in combination with negative electrodes (based on only ACs) for the realization of complete lithium-ion capacitors.

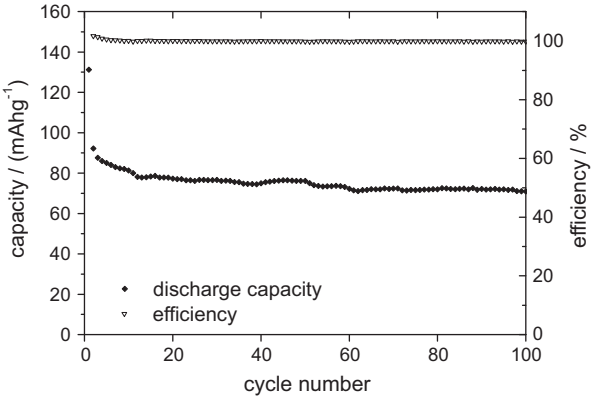

Fig. 8. Cycling performance of a $LiFePO_4$/AC electrode (IV) during a 50C–1D test.

4. Conclusion

Composite electrodes containing $LiFePO_4$ and AC as active materials and CMC as binder appear extremely promising for the development of high performance Li-ion capacitors.

As shown with the C-rate tests, electrodes containing 65 wt.% $LiFePO_4$, 20 wt.% AC, 10 wt.% Super P are able to display specific capacities of almost 140 mAh g^{-1} (at a charge current density corresponding to 20C) with very high cycling stability. When subjected to 5C–1D cycles, these electrodes exhibited a discharge capacity of ca. 140 mAh g^{-1} with a capacity fading lower than 0.02% per cycle after 500 cycles. In addition, these electrodes displayed extremely promising performance also during prolonged pulse tests by delivering 60 mAh g^{-1} after 100 cycles with pulsed charge of 100C. Moreover, the applied pulsed charge did not cause any damage in the electrodes, as indicated by the fact that the 1C–1D electrode performance before and after the pulsed charge was identical. Finally, during CC tests at 50C–1D the electrodes displayed a capacity of ca. 70 mAh g^{-1} for 100 cycles.

Finally, we also showed that the combined used of two common and low price materials, like AC and Super P, leads to a significant increase of conductivity of $LiFePO_4$ based electrode.

Acknowledgments

The authors wish to thank the Westfälische Wilhelms Universität Münster and the Ministerium für Innovation, Wissenschaft, Forschung und Technologie des Landes Nordrhein-Westfalen (MIWFT) for the financial support. We gratefully appreciated the supply of materials by Süd-Chemie AG ($LiFePO_4$), Norit Activated Carbon Holding (AC) and TIMCAL (Super P).

References

[1] P. Simon, Y. Gogotsi, Nat. Mater. 7 (845) (2008).
[2] A. Du Pasquier, I. Plitz, J. Gural, F. Badway, G.G. Amatucci, J. Power Sources 136 (160) (2004).
[3] X. Hua, Z. Denga, J. Suoa, Z. Pan, J. Power Sources 187 (635) (2009).
[4] X. Hu, Y. Huai, Z. Lin, J. Suo, Z. Deng, J. Electrochem. Soc. 154 (A1026) (2007).
[5] K. Striebel, J. Shim, A. Sierra, H. Yang, X.Y. Song, R. Kostecki, M. McCarthy, J. Power Sources 146 (33) (2005).
[6] G. Arnorld, J. Garche, R. Hemmer, S. Ströbele, C. Vogler, M. Wohlfahrt-Mehrens, J. Power Sources 119–121 (247) (2003).
[7] A.G. Pandolfo, A.F. Hollenkamp, J. Power Sources 157 (11) (2006).
[8] S.F. Lux, F. Schappacher, A. Balducci, S. Passerini, M. Winter, J. Electrochem. Soc. 157 (A320) (2010).
[9] V. Ruiz, A.G. Pandolfo, Electrochchim. Acta 55 (7495) (2010).
[10] N. Ravet, Y. Chouinard, J.F. Magnan, S. Besner, M. Gauthier, M. Armand, J. Power Sources 97–98 (503) (2001).
[11] Z. Chena, J.R. Dahn, J. Electrochem. Soc. 149 (A1184) (2002).
[12] V. Palomares, A. Goni, I.G. de Muroa, I. de Meatza, M. Bengoechea, I. Cantero, Teófilo Rojoa, J. Power Sources 195 (7661) (2010).
[13] V. Srinivasan, J. Newman, Electrochem. Solid-State Lett. 9 (A110) (2006).
[14] I.V. Thorat, V. Mathur, J.N. Harb, D.R. Wheeler, J. Power Sources 162 (673) (2006).
[15] B. Jin, E.M. Jin, K.-H. Park, H.-B. Gu, Electrochem. Commun. 10 (1357) (2008).